Title

Hypoxia Mimicking Hydrogels to Regulate the Fate of Transplanted Stem Cells

Authors

Binulal N. Sathy[1,2], Andrew Daly[1,2], Tomas Gonzalez-Fernandez[1,2,4,] Dinorath Olvera[1,2], Grainne Cunniffe[1,2], Helen O. McCarthy[6], Nicholas Dunne[1,2,5,6], Oju Jeon [7,8,9], Eben Alsberg[7,8,9], Tammy H. Donahue[10,11], Daniel J. Kelly[1,2,3,4]

Affiliations

[1]Trinity Centre for Bioengineering, Trinity Biomedical Sciences Institute, Trinity College Dublin, Dublin, Ireland.

[2]Department of Mechanical and Manufacturing Engineering, School of Engineering, Trinity College Dublin, Dublin, Ireland.

[3]Department of Anatomy, Royal College of Surgeons in Ireland, Dublin, Ireland.

[4]Advanced Materials and Bioengineering Research Centre (AMBER), Royal College of Surgeons in Ireland and Trinity College Dublin, Dublin, Ireland.

[5] Centre for Medical Engineering Research, School of Mechanical and Manufacturing Engineering, Dublin City University, Dublin, Ireland.

[6] School of Pharmacy, Queen's University Belfast, 97 Lisburn Road, Belfast BT9 7BL, UK.

[7] Department of Biomedical Engineering, Case Western Reserve University, Cleveland, USA.

[8] Department of Orthopaedic Surgery, Case Western Reserve University, Cleveland, USA.

[9] National Centre for Regenerative Medicine, Case Western Reserve University, Cleveland, USA.

[10] School of Biomedical Engineering, Colorado State University, Fort Collins, CO, USA.

[11] Department of Mechanical Engineering, Colorado State University, 1374 Campus Delivery, Fort Collins, CO 80523, USA.

Abstract

Controlling the phenotype of transplanted stem cells is integral to ensuring their therapeutic efficacy. Hypoxia is a known regulator of stem cell fate, the effects of which can be mimicked using hypoxia-inducible factor (HIF) prolyl hydroxylase inhibitors such as dimethyloxalylglycine (DMOG). By releasing DMOG from mesenchymal stem cell (MSC) laden alginate hydrogels, it is possible to stabilize HIF-1α and enhance its nuclear localization. This correlated with enhanced chondrogenesis and a reduction in the expression of markers associated with chondrocyte hypertrophy, as well as increased SMAD 2/3 nuclear localization in the encapsulated MSCs. *In vivo,* DMOG delivery significantly reduced mineralisation of the proteoglycan-rich cartilaginous tissue generated by MSCs within alginate hydrogels loaded with TGF-β3 and BMP-2. Together these findings point to the potential of hypoxia mimicking hydrogels to control the fate of stem cells following their implantation into the body.

1. Introduction

The clinical success of stem cell-based therapies largely depends on the ability to control stem cell fate *in vivo*. Stem cells sense and respond to the biochemical signals and biophysical forces they experience in their local environment [1] . Oxygen availability has been identified as a key determinant of numerous stem cell functions including proliferation, maintenance of stemness and cell-fate commitment [2]. Oxygen levels have also been shown to regulate chondrogenesis, osteogenesis and adipogenesis of mesenchymal stem cells (MSCs) and to modulate their paracrine functions [3-7]. Therefore, engineering implantable devices that can control local oxygen levels, or mimic the effects of instructive oxygen environments, may be key to regulating the fate of stem cells in vivo.

Hypoxia inducible factors (HIFs) are transcriptional activators comprised of the constitutively expressed β subunit (HIF-1β) which binds with one of the hypoxia inducible α subunits (HIF-1α or HIF-2α) to regulate cell response to changes in oxygen tension [8, 9] . Dysregulation of HIFs has been shown to be associated with many pathological processes, while therapeutic modulation of HIFs is gaining increased interest for the treatment of different diseases [9]. In recent years, several small molecules have been developed which can inhibit HIFs at the gene or protein level [10, 11] . HIF prolyl hydroxylases (HIF PH) regulate the HIF transcriptional cascade in response to differences in oxygen availability [12, 13]. In low oxygen environments, degradation of the HIF-α subunits through the ubiquitin-proteosomal pathway initiated by oxygen and iron-dependent HIF-PH is inhibited. As a result, α subunits accumulate and translocate to the nucleus where they dimerize with β subunits and influence downstream signalling. Pharmacological inhibition of HIF-PH by the cell penetrating compound dimethyloxalylglycine (DMOG) can

mimic the effect of low oxygen conditions by stabilizing HIF-1α and inducing HIF-1 dependent transcription of downstream genes [13, 14].

Oxygen levels are known to strongly regulate the differentiation of mesenchymal stem cells (MSCs) [3, 5, 15-18]. A low oxygen tension is known to enhance chondrogenesis of MSCs and to inhibit hypertrophy and progression along an endochondral pathway [7, 19]. Either hypoxia or HIF-1a overexpression has been shown to be effective and sufficient to induce chondrogenesis of MSCs[19], while HIF-1α has been shown to potentiate BMP2-induced cartilage formation and inhibit endochondral ossification during ectopic bone/cartilage formation [20]. A number of studies have also demonstrated that HIF stabilizing compounds can enhance chondrogenesis of MSCs [19, 21, 22], with a recent comparison of three such compounds demonstrating that DMOG stimulation induce a more chondrogenic transcriptional profile [23].

Different biomaterial-based systems have been developed in an attempt to control the fate of stem cells. Modulation of biomaterial composition, stiffness [24, 25], scaffold pore size [26] and the local delivery of recombinant proteins [27, 28]have all been explored as strategies to regulate stem cell differentiation *in vitro* and *in vivo*. Despite the known importance of oxygen levels in regulating the fate of cells, relatively few biomaterial systems have been developed to modulate the oxygen environment or mimic the effects of altered oxygen conditions. Attempts have been limited to the development of hypoxia-inducible hydrogels that form hydrogel networks via oxygen consumption [29, 30] , cobalt ion releasing scaffolds to mimic the effect of hypoxia to enhance angiogenesis for bone tissue engineering [31, 32] and oxygen generating/delivering biomaterials [33, 34]. This study reports the development of a hydrogel system to deliver a prolyl-hydroxylase inhibitor to MSCs, which functions to stabilize HIF-1α in the encapsulated

cells. When coupled with controlled growth factor delivery, we demonstrate that such biomaterial systems can be used to modulate the differentiation of transplanted MSCs *in vivo*.

2. Materials and Methods

2. 1 MSC isolation, expansion and encapsulation within the RGD-alginate hydrogels

MSCs were isolated and expanded from the femoral shaft of 4-month-old pigs as previously reported. Briefly, aseptically harvested mononuclear cells from the femur were diluted in Dulbecco's modified Eagle's medium with GlutaMAX (here after known as expansion medium) supplemented with 10% v/v foetal bovine serum (FBS), 100 U mL^{-1} penicillin/100 μg mL^{-1} streptomycin (all Gibco Biosciences, Ireland) and 5 ng mL^{-1} human fibroblastic growth factor-2 (FGF-2; Prospec-Tany TechnoGene Ltd., Israel) and seeded on to T175 tissue culture flasks at a seeding density of 1.5 x 10^5 cells/cm^2. Non-adherent cells were washed away after 24 h and MSCs attached to the tissue culture flask were allowed to develop colonies. MSC colonies were trypsinised at nearly 70% confluency and reseeded with a density of 5 x10^3 cells per cm^2 on T175 flasks, expanded in 20% O_2 and cryopreserved in liquid nitrogen. The colony forming unit assay (CFU-F) of isolated MSCs were evaluated (data not shown) and passage 2-3 cells from the same donor was used for all experiments in this study.

Sodium alginate powder (MW=196000 Da) (Pronova Biopolymers, Norway) was gamma-irradiated (5 Mrad) [35] and RGD (GGGGRGDSP) peptides were covalently coupled to alginate (10 mg RGD per g of alginate) with aqueous carbodiimide chemistry, purified and sterilised as previously described [36, 37]. In brief, sterile RGD-alginate solution (4 wt.%) was prepared by overnight stirring of alginate in ultrapure water in a 50-mL falcon tube. Single cell suspension of

MSCs was prepared in the expansion media and mixed with the alginate solution in 1:1 ratio and a 2% RGD-alginate solution containing MSCs were prepared. Sterile agarose (Sigma-Aldrich, Ireland) (3%) containing 50 mM calcium chloride (Sigma-Aldrich, Ireland) was prepared and custom-made agarose moulds containing multiple wells (5 mm dia. x 3 mm depth) were prepared. MSCs encapsulated within RGD-γ-alginate hydrogels (5 mm dia. x 3 mm depth) were prepared by pipetting the MSCs containing alginate-gel solution in to the wells in the agarose mould and incubating it for 15-20 min at 37^{o} C. The prepared hydrogels were maintained in chondrogenic growth media without FBS, supplemented with 100 µg mL-1 sodium pyruvate, 40 µg mL-1 L-proline, 50 µg mL-1 L-ascorbic acid-2-phosphate,1.5 mg mL-1 bovine serum albumin, 1X insulin-transferrin-selenium, 100 nM dexamethasone (all from Sigma-Aldrich, Ireland) and 10 ng mL-1 recombinant human TGF-β3 (ProSpec-Tany TechnoGene Ltd., Israel) unless stated otherwise. For specifically investigating the role of GFs encapsulated within the hydrogels, Chondrogenic growth media without TGF-β3 supplementation was used for specifically investigate the role of GFs encapsulated within the hydrogels in chondrogenesis of MSCs in the presence and absence of DMOG. Defined oxygen conditions (20 % O2 or 5% O2) for the experimental conditions were provided using normoxia and hypoxia CO2 incubators (Steri-Cycle, Thermo Fisher Scientific, UK New Brunswick™ Galaxy® 170R, Eppendorf, UK) and media change was performed every other day. In order to minimise the changes in the oxygen conditions in the case of 5% O2, growth media maintained in 5% oxygen incubator in cell culture flasks was used during media changes and media change was performed as quick as possible.

2.2 Preparation of DMOG delivery hydrogels and DMOG and GF co-delivery hydrogels

DMOG delivery hydrogels were prepared by incorporating three different concentrations of DMOG (Sigma-Aldrich, Ireland) (2.1, 4.2 and 6.3 mg/mL) into the RGD-alginate hydrogel solutions before mixing with MSCs. Release profiles of DMOG from the hydrogels were evaluated using ultraviolet (UV) spectrometry as previously reported [38]. Briefly, DMOG-loaded RGD-alginate hydrogels containing MSCs was incubated in 2 mL OptiMEM (Sigma-Aldrich, Ireland) at 37 °C for defined time periods (1, 3, 6, 24, 48 and 72 h). At each time point, 1 mL of media was collected from the well for analysis and 1 mL fresh media was added back to the well. The absorbance maxima of DMOG in the media was reconfirmed by scanning the media containing increasing concentrations of DMOG from 200 to 300 nm at 1 nm intervals. The absorption maxima was confirmed as 230 nm (Supplementary Fig. 1). The cumulative release of DMOG from the hydrogel was calculated by using increasing concentrations of DMOG as standards. The GF delivery hydrogels were prepared by incorporating previously reported optimal concentrations of BMP-2 (400 ng/mL) and TGF-β3 (40 ng/mL) [39] to the RGD-alginate. The DMOG co-delivery hydrogels were prepared by combining 4.2 mg/mL of DMOG (final concentration in the RGD alginate) with the GF incorporated RGD-alginate just before preparing hydrogels. MSCs were encapsulated in this hydrogel solution at a density of 10 million/mL and hydrogels were prepared as described above.

2.3 Viability of MSCs encapsulated in DMOG delivery hydrogels

Viability of MSCs encapsulated within the DMOG delivery hydrogels was evaluated at 24 h using live/dead assay kit (Invitrogen, Dublin, Ireland) as per the manufacture's instructions. Briefly, MSCs encapsulated DMOG delivery hydrogels were maintained in the growth media for 24 h in the incubator. After 24 h, these hydrogels were incubated in optiMEM containing 20 mM Calcein and 5 mM Ethidium bromide for 30 min at 37^{o} C. After 30 min of incubation, hydrogels

were washed three times in fresh OptiMEM and were imaged using the confocal microscope (TCS SP8 II; Leica Microsystems, Mannheim, Germany) with laser power, gain and offset conditions optimised with positive and negative controls. Metabolic activity of the encapsulated cells was evaluated at day 1, 3 and 7 using alamar blue assay (alamarBlue™ Cell Viability Reagent, Invitrogen) as per manufactures instructions. In order to evaluate the proliferation of the cells encapsulated within the hydrogels, DNA content at day 1, 3 and 7 were evaluated using Hoechst Bisbenzimide 33258 dye assay (Quant-iT ssDNA Assay Kit, Biosciences).

2.4 HIF stability and nuclear translocation in MSCs encapsulated within the hydrogels

For evaluating HIF stability and its nuclear translocation in MSCs, both immunofluorescence staining and western blot analysis were performed after encapsulating MSCs in DMOG delivery hydrogels at 2h and 24h respectively. For immunofluorescence staining, MSCs in the hydrogels were fixed with 4% paraformaldehyde for 20 min at room temperature. After fixation, the hydrogels were pooled (minimum 6 numbers) incubated in 55 mM sodium citrate solution for 30 min and MSCs were separated from the gel network. After 30 min, cells were centrifuged down and permeabilized using 0.5 % Triton-X 100 (Sigma-Aldrich, Ireland) for 5 min. After that, cells were blocked with 1% bovine serum albumin (BSA) for 1 h. Blocked cells were incubated in mouse monoclonal anti-HIF-1α antibody, (Abcam, Cambridge, UK) prepared in 1% BSA (1:1000 dilution) and were incubated overnight at 4^{o}C. After overnight incubation, cells were washed in PBS and MSCs were collected by centrifugation. FITC- conjugated goat anti-mouse secondary antibody (Abcam, Cambridge, UK) prepared in the blocking buffer (1:2000 dilution) was added to the cells and were incubated for 1 h. After 1h incubation, MSCs were washed 3 times and counterstained with DAPI (VWR, Ireland) for 5 min. Then, the stained cells were

dropped on the confocal dishes and were imaged using confocal microscope and analysed as previously reported as previously reported [34]. The laser power, gain and offset of the microscope was kept constant in between the groups to minimize error. For calculating the signal intensity of our region of interest, the total cell area visible was outlined and the mean grey signal intensity value was recorded using Image J. High resolution images were acquired for FITC and DAPI by sequential scanning using the Leica (SP-8 Germany) confocal microscope. A minimum of 50 cells were analyzed for each group for quantitative assessment.

For western blot analysis, hydrogels containing MSCs were transferred to in Eppendorf tubes containing ice cold RIPA buffer (50 mM Tris-HCl pH 8.0, 150 mM sodium chloride, 1.0% Triton X-100, 0.1% SDS, with 1% protease inhibitor cocktail, all from Sigma-Aldrich, Ireland) 24 h after encapsulating MSCs within the hydrogels. Tubes were kept on ice and the gels were mechanically disrupted using an 18 G needle and a micro pestle. The resulting solution was centrifuged at 15,000 g for 15 min to remove cell and hydrogel debris from the solution. Total protein concentration was quantified using the BCA assay. Samples were diluted in laemmli sample buffer and proteins were denatured by heating to 95^{O}C under reducing conditions. After denaturation, proteins were separated on 8% SDS polyacrylamide gels and transferred to PVDF (Millipore, Ireland) membranes. Membranes were blocked with 5% BSA (bovine serum albumin) in tris-buffered saline containing 0.1% TSB-T (Tween 20) and probed with anti HIF-1 α antibody (Abcam, Cambridge, UK) (Dilution 1:2000). Membranes were washed five times with TBS-T and treated with anti-rabbit peroxidase conjugated secondary antibody (Abcam, Cambridge, UK) in 5% BSA-TBS-T (Dilution 1:5000). Blots were developed using an enhanced chemiluminescent substrate (Millipore, Ireland) and protein bands were visualized and imaged using a chemiDoc imaging system (Biorad, UK)

2.5 Nuclear translocation of Smad 2/3 in MSCs encapsulated within the hydrogels

For evaluating Smad 2/3 nuclear translocation in MSCs, hydrogels maintained in 5% O_2 and 20% O_2 were harvested at 48 h and fixed with 4% paraformaldehyde for 20 min at room temperature. Then the hydrogels were pooled (minimum 6 numbers) and incubated in 55 mM sodium citrate solution for 30 min followed by centrifugation. Recovered cells were permeabilized and blocked as described above (2.4). Blocked cells were incubated in Smad 2/3 rabbit polyclonal antibody (Santa Cruz, UK), prepared in 1% BSA (1:500 dilution) and were incubated overnight at 4^{o}C. After overnight incubation, cells were washed in PBS and MSCs were collected by centrifugation. FITC- conjugated goat anti-rabbit secondary antibody (Santa Cruz, UK) prepared in the blocking buffer (1:2000 dilution) was added to the cells and were incubated for 1 h. Then the cells were counter stained with DAPI and high-resolution images were acquired and analysed as described above (2.4).

2.6 Quantitative PCR analysis of gene expression in MSCs encapsulated within the hydrogel.

Day 0 and day 7 hydrogels (n=5 gels/group/time point) were transferred to RNase-free 2 mL microtubes containing β-mercaptoethanol (Sigma-Aldrich, Ireland) supplemented (10 µl mL^{-1}) RLT buffer (Qiagen, UK). Tubes were kept in ice and hydrogels were mechanically disrupted using RNase-free needles and a micro-pestles and were stored in -80^{o}C until used for RNA isolation. For RNA isolation, this lysate was thawed on ice and homogenized using a QIAshredder column (Qiagen, UK) just before the isolation procedure. Total RNA was isolated and purified using the RNeasy mini kit (Qiagen, UK) using the manufacturer's suggested protocol. The purity and yield of RNA were quantified using a NanoDrop Spectrophotometer (Labtech International, UK). A total of 50 ng RNA per sample was reverse transcribed per 20 µL

reaction volume of a high capacity reverse transcription cDNA kit (Applied Biosystems, UK) as per manufacturer's instructions to obtain high quality cDNA. Quantitative PCR was performed using SYBR select master mix (Applied Biosystems, UK) using ABI 7500 sequence detection system (Applied Biosystems, UK). The relative expression of type-I collagen (Col-1), type-II collagen (Col-2), type-X collagen (Col-10), aggrecan (ACAN), matrix metallopeptidase-13 (MMP-13), osteopontin (OPN) and glyceraldehyde-3-phosphate dehydrogenase (GAPDH) were analyzed. Primer sequences, (KiCqStart® SYBR® Green Primers; Sigma, Ireland) used for amplification of genes are listed in Table 1. Comparative Threshold (cT) data were analyzed using the ΔΔCT method as described previously [40] with GAPDH values from the respective oxygen tension as the endogenous control. Relative expression of the genes is presented as fold changes relative to the control group from the respective oxygen tension.

2.7 Subcutaneous implantation of MSC laden hydrogels in nude mice

Animal experiments were conducted after obtaining approval by the institutional ethics committee and the Irish Medicines Board (IMB), approval number AE 19136/P0324. The potential of DMOG delivery hydrogels to modulate stem cell fate *in vivo* was evaluated at 4 weeks and 12 weeks. Hydrogels were implanted into the subcutaneous space of Balb/C nude mice (Harlan, UK) using a previously described surgical procedure[41]. In brief, two subcutaneous pockets (one in the shoulder level and one in the hip level) were created per animal in the dorsal side of the animal under aseptic conditions. Next, three hydrogel-cell constructs were implanted per pocket (six per mouse) n = 8 per group. Constructs after the study period were evaluated based on the gross appearance, micro computed tomography (μCT) scan, histology and immunohistochemistry.

2.8 Biochemical analysis for sulphated glycosaminoglycan (sGAG) and collagen content

Hydrogels were stored at ˉ80^{o}C until digested with papain enzyme as previously reported[42]. Briefly, papain buffer extract (PBE) was prepared using 100 mM sodium phosphate buffer containing 0.1 M sodium acetate, 0.05 M ethylenediaminetetra-acetic acid, (all from Sigma-Aldrich, Ireland) and the pH of the solution was adjusted to 6.0. To this buffer, 125 μg mL^{-1} papain (Sigma-Aldrich, Ireland) was added and was activated with 10 mM cysteine hydrochloride immediately before usage. DNA content in the papain digested samples was quantified using Hoechst Bisbenzimide 33258 dye assay (Quant-iT ssDNA Assay Kit, Biosciences). sGAG levels in the samples were measured using dimethylmethylene blue dye-binding assay, pH 1.35 (Blyscan, Biocolor Ltd., UK) as previously described[42]. For the collagen assay, papain digested samples were hydrolysed by treating with concentrated HCL (37%) and collagen content in the samples was quantified by measuring their hydroxyproline content using the Chloramine-T assay. Collagen and sGAG content in the constructs were normalised with DNA content in the samples.

2.9 μCT analysis

A high resolution μCT imaging system Scanco Medical 40 (Scanco Medical, Bassersdorf, Switzerland) with 70 kVp X-ray source and 112 μA (resolution of ~12μm) was used for scanning the constructs. To evaluate the potential of the hydrogels to suppress mineralization, μCT scans were performed at 12 weeks on DMOG releasing and control hydrogels. Volumetric reconstructions and analysis of the acquired data were performed by analysis and visualization software provided along with the imaging system. A cylindrical volume covering the entire construct was selected as the volume of interest (VOI) and a global threshold of 70–255 was

used for analysing all the constructs. Reconstructed 3D images generated from the scans were used to visualize mineral distribution throughout the constructs and quantitative measurements were expressed as mineral volume within the VOI.

2.10 Histological and immunohistochemical evaluation of the constructs

Hydrogel-cell constructs were fixed in 4% paraformaldehyde (Sigma-Aldrich, Ireland) at the end of each study period, dehydrated and were wax embedded. Seven-µm thick sections were obtained from the paraffin embedded samples using a microtome (Leica, Germany). Sections were stained with aldehyde fuchsin/alcian blue (AF/AB) for visualizing sGAG, standard picrosirius red (PSR) for evaluating the collagen deposition. For type-1 collagen and type-2 collagen immunostaining, antigen retrieval was carried out on the sections by pre-treating them with pronase (Sigma-Aldrich) at 37 °C for 5 min in a humidified environment. Then, sections were blocked with goat-serum (Sigma-Aldrich) for 1 h and incubated with mouse monoclonal type-2 anti-collagen antibody primary antibody (all Abcam, Cambridge, UK). After overnight incubation, sections were washed in PBS and incubated with the secondary antibody, goat anti-mouse IgG (B7151, Sigma) for 1 h. Color was developed using the Vectastain ABC reagent kit (Vectastain ABC kit, Vector Laboratories, UK) followed by exposure to DAB peroxidase substrate (DAB Peroxidase (HRP) Substrate Kit, Vector Laboratories, UK). Reaction was stopped when colour was visible and sections were washed, dehydrated through alcohol gradient and mounted using Vectashield (Vector Laboratories, UK).

2.11 Statistical analysis

Statistical analyses were performed by GraphPad Prism software (v.6, GraphPad, USA). Quantitative findings are presented as mean ± standard deviation. Student's t-test was used to

compare differences between two experimental groups and oneway analysis of variance (ANOVA) with Tukey post-hoc test was used to make pairwise comparisons between multiple groups. Statistical significance was set to $p<0.05$.

3. Results

3.1 DMOG releasing hydrogels stabilize HIF-1α in MSCs

The cell penetrating compound dimethyloxalylglycine (DMOG) has been shown to mimic the effects of hypoxia by stabilizing HIF-1α [7, 19, 43, 44]. We first sought to determine if an RGD modified alginate hydrogel could be used as a delivery system to expose encapsulated MSCs to DMOG during the early stages of differentiation. To this end we evaluated the release kinetics of different initial doses of DMOG from alginate hydrogels. For all doses, a burst release of DMOG was observed from the hydrogel over the first 3 hrs followed by a slower but sustained release for a period of 72h (Fig. 1A), with 80-100% of the loaded DMOG released over this 72-hour period. MSCs encapsulated within the hydrogels remained viable irrespective of the amount of DMOG added to the construct (Fig.1B). There was a significant decrease in the metabolic activity of MSCs encapsulated within the DMOG releasing hydrogels at day 1 and 3 (Supplementary Figure 2), but by day 7 there were no significant difference compared to control conditions. There was no significant change in the DNA content of MSC laden hydrogels overtime or between the groups (Supplementary figure-2). To assess if DMOG delivery from alginate hydrogels was leading to HIF-1 stabilization in encapsulated cells, HIF-1α levels in the nucleus of MSCs encapsulated in RGD-Alginate (control) and DMOG releasing RGD-Alginate (4.2 mg DMOG /mL) hydrogels maintained at either normoxia (20% O_2) or low oxygen condition (5% O_2) (Fig. 1C) were evaluated using confocal microscopy. Two hours post-

encapsulation, the ratio of nuclear to cytoplasmic HIF-1α was higher in MSCs encapsulated within HIF-stabilizing hydrogels maintained at 20% O_2 compared to control constructs (Fig. 1D). In contrast, no statistically significant difference in nuclear HIF-1α levels were observed in constructs maintained at 5% O_2 (Fig. 1D). 24 hours post-encapsulation, western blot analysis confirmed stabilization of HIF-1α within MSCs encapsulated in DMOG releasing hydrogels which were maintained at both 5 % and 20% O_2 (Fig. 1E).

3.2 DMOG delivery enhances chondrogenesis and supresses hypertrophy

Oxygen availability is believed to play a key role in long bone development by regulating HIF-1α and HIF-2α signalling in stem cells and activating chondrogenesis [3, 13, 19, 23] . To determine if DMOG delivery and associated regulation of nuclear HIF-1α levels could regulate the differentiation of adult stem cells, DMOG releasing hydrogels (RGD-alginate containing either 2.1, 4.2 and 6.3 mg DMOG /mL) containing MSCs were maintained in culture in the presence of TGF-β3, a growth factor known to play a crucial role in skeletal development [45]. When maintained in a normoxic environment (20% O_2), DMOG releasing hydrogels enhanced the expression of key chondrogenic genes such as type-II collagen (Col-2) and aggrecan, and supressed expression of the hypertrophic marker matrix metallopeptidase-13 (MMP-13) for all the three DMOG concentrations (Fig. 2A) under standard chondrogenic media conditions. At 20% oxygen, DMOG release did not significantly influence the expression of type I collagen (Col-1), but the expression of type X collagen (Col-10) significantly increased for the lowest concentration of DMOG delivery. The expression of the osteogenic marker osteopontin was significantly reduced at medium and higher concentrations of DMOG delivery in 20 % oxygen conditions. When maintained at low oxygen conditions (5% O_2), no significant changes in Col-1, Col-10 or osteopontin gene expression were observed in DMOG releasing hydrogels. In such

low oxygen conditions, hydrogels releasing high concentrations of DMOG were found to supress type II collagen (Col-2) expression but to continue promoting aggrecan gene expression. The highest concentration of DMOG significantly down regulated MMP-13 expression (Fig. 2B).

We next assessed if these short term (week 1) changes in gene expression would lead to longer term (week 3) changes in tissue development within DMOG releasing hydrogels. When maintained at 20% O_2, DMOG release enhanced type-II collagen deposition, although glycosaminoglycan production did not significantly increase (Fig. 2C-G). In agreement with the literature [3, 18, 46], chondrogenesis was enhanced in hydrogels maintained at 5% O_2 as evident by increased sGAG and type II collagen deposition. In such low oxygen conditions, DMOG release was found to significantly increase GAG accumulation (Fig. 2D and F), although no differences in overall collagen deposition was observed (Fig. 2C and E). Even though decreases in col-2 gene expression was observed after 1 week in a low oxygen environment, intense type-II collagen deposition was observed at the protein level in all DMOG releasing hydrogels at week 3. Type-II collagen deposition appeared to be more diffuse throughout the matrix in DMOG containing hydrogels, but more localized to the pericellular space in in the control constructs (Fig. 2G).

3.3 DMOG delivery increases Smad 2/3 nuclear translocation

Smads are known to play a central role in regulating chondrogenesis and osteogenesis of MSCs [47, 48]. Members of the TGFβ subfamily ligands, by binding and assembling a receptor complex on the cell, activate and transduce downstream signalling through receptor smads (R-Smads) 2 and 3 [47, 48]. To better understand the mechanism by which these hypoxia mimicking hydrogels were enhancing chondrogenesis of encapsulated MSCs, we next investigated Smad 2/3

levels and their nuclear translocation in DMOG releasing hydrogels (Fig. 3A, B). A clear increase in Smad 2/3 levels was observed in MSCs maintained at 5% O_2 (Fig. 3C). DMOG releasing hydrogels were also found to increase nuclear Smad 2/3 levels in MSCs maintained at both 20% and 5% oxygen (Fig. 3D, E).

3.4 Co-delivery of DMOG, TGF-β3 and BMP-2 initiates chondrogenesis

Co-delivery of TGF beta and BMP-2 from alginate hydrogels has been previously shown to promote endochondral bone formation *in vivo* [39, 49]. With a view towards assessing if DMOG delivery could be used to modulate MSC fate *in vivo,* we first examined how co-delivery of DMOG, TGF-β3 and BMP-2 would impact MSC differentiation *in vitro*. Co-delivery of these factors was found to enhance chondrogenesis compared to delivery of DMOG or growth factors (GFs) in isolation when constructs were maintained at 20% oxygen (Fig. 4). Specifically, co-delivery increased the expression of the early chondrogenic markers Sox-9, type II collagen and type X collagen at 20% oxygen, in media not additionally supplemented with TGFβ-3. In the same media conditions, in already low oxygen conditions (5% oxygen), DMOG delivery had no effect on the expression of chondrogenic marker genes Sox-9, Col-2 and aggrecan. After 4 weeks *in vitro,* DMOG and GF releasing hydrogels contained higher levels of GAGs compared to all other groups (Fig. 4C). Short-term delivery of DMOG from the hydrogel did not negatively influence collagen production within the hydrogels (Fig. 4 D).

3.5 DMOG delivery modulates transplanted stem cell fate *in vivo*

To assess how DMOG delivery influences MSC fate *in vivo*, we subcutaneously implanted GF (40 ng/mL TGF-β3 and 400 ng/mL BMP-2) or GF and DMOG (4.2 mg/mL) releasing hydrogels (co-delivery) containing MSCs into the subcutaneous space of nude mice and evaluated tissue

development after 4 and 12 weeks. After 4 weeks *in vivo*, both hydrogels supported the development of a fibrocartilaginous-like tissue, as evident by the deposition of sGAG and type-I and type-II collagen (Fig. 5A). Furthermore, type X collagen deposition was also observed after 4 weeks *in vivo* (Fig. 5F). Type-I collagen deposition appeared more intense in GF releasing hydrogels compared to constructs containing both DMOG and GF (Fig. 5A). GF + DMOG releasing hydrogels appeared denser than GF releasing hydrogels, the central regions of which appeared more porous and disrupted. Differences in tissue development within the two hydrogel systems became more evident with time *in vivo*. After 12 weeks, the GF-delivery hydrogels supported the development of an early bone-like tissue as evident by H&E and Goldner's trichome staining and areas of mineral deposition within the constructs (Fig. 5B). In contrast, negligible mineral deposition was observed in DMOG + GF delivery hydrogels (Fig. 5B). This was confirmed by μCT analysis which demonstrated higher levels of mineral deposition within GF hydrogels. The GF + DMOG releasing hydrogels appeared to support the development of a more stable cartilaginous tissue, with higher levels of sGAG accumulation (Fig. 5C), which appeared to prevent the degradation of the hydrogel construct *in vivo*. This demonstrates the potential of DMOG-releasing hydrogels to modulate MSC differentiation *in vivo*, supporting the development of a more stable, cartilage-like tissue as opposed to the default phenotype of chondrogenically primed MSCs *in vivo* which is to proceed along an endochondral pathway.

4 Discussion

In this study we used alginate hydrogels to deliver DMOG to MSCs, where both the compound and the cells were encapsulated into the hydrogel at the time of fabrication. DMOG acts by

regulating the activity of two hydroxylases, prolyl hydroxylase 2 and factor inhibiting HIF, that determine the participation of HIF-1α subunit in the HIF complex [50]. During the first 72 hours after hydrogel fabrication, the majority of DMOG was released from the alginate hydrogel, providing encapsulated cells with short-term exposure to this compound. Alginate has been previously used as a drug delivery system, especially for short-term drug release[51]. Encapsulation of MSCs into the alginate hydrogel facilitates the localized delivery of DMOG to the encapsulated cells, which would be difficult to control using, for example, bolus injection of the compound to a site of injury. As expected, DMOG stimulation was found to stabilize HIF-1α in MSCs, which correlated with increased nuclear Smad 2/3 levels and ultimately enhanced MSC chondrogenesis and a suppression of hypertrophy. When combined with growth factor delivery, these hypoxia mimicking hydrogels were found to promote a more stable chondrogenic phenotype *in vivo*, as evident by a reduction in cartilage matrix calcification compared to hydrogels that did not contain DMOG.

In agreement with recent studies [23], DMOG was found to stabilize HIF-1α in MSCs. Indeed, DMOG delivery appeared to have greater effect on HIF-1α stabilization than lowering the external oxygen concentration from 20% to 5%. This is perhaps unsurprising, as 5% O_2 can be considered as more physiological for tissues such as articular cartilage, with lower oxygen conditions likely required to promote a hypoxic response. Other studies have reported improved chondrogenesis at <3% oxygen compared to higher oxygen tensions, which could be correlated to increased HIF stabilization at <3% O2 [46, 52, 53]. Previous studies have observed that that HIF-1α can improve chondrogenesis by inducing type-2 collagen expression through the interaction with the Sox 9 promoter [53, 54]. It has also been shown that HIF-1α overexpression is effective and sufficient to induce chondrogenesis of MSCs without the use of exogenous

growth factors[19], although we found that DMOG stimulation in the absence of exogenous TGF-β did not result in robust chondrogenesis.

We found that short-term exposure to DMOG can lead to long term changes in the phenotype of MSCs both *in vitro* and *in vivo*, including changes in chondrogenic gene expression at week 1 (*in vitro*), increases in cartilage-specific matrix accumulation at week 3 (*in vitro*) and a more stable cartilage-like phenotype after 12 weeks *in vivo*. We were initially concerned that DMOG exposure might supress collagen synthesis, as 2-oxoglutarate analogues such as DMOG can also inhibit prolyl 4-hydroxylases that play a crucial role in collagen biosynthesis [43]. Indeed, treating articular chondrocytes with DMOG has previously been shown to increase Sox-9 expression but to supress type II collagen expression [43]. However, in our study, DMOG release from the hydrogels did not appear to affect long-term collagen bio-synthesis, which may be due to its relatively fast release and clearance from the hydrogel (~80-100 % of the loaded DMOG is released within 72 hours of encapsulation). Further emphasising the importance of temporal DMOG exposure on chondrogenesis of MSCs, recent studies have found that sustained DMOG stimulation is found to suppress type II collagen expression [23]. While we did observe that DMOG delivery led to reduced type II collagen gene expression after 1 week of culture, no long-term changes in type II collagen deposition were observed. This suggests that short-term delivery of DMOG from alginate hydrogels can lead to long term improvements in chondrogenesis with no negative effects on long-term collagen synthesis.

DMOG releasing hydrogels were found to increase nuclear Smad 2/3 levels in MSCs maintained at both 20% and 5% oxygen, suggesting that increases in MSC chondrogenesis and the suppression of hypertrophy within these constructs can be linked to increases in nuclear SMAD 2/3. Smads are known to play a central role in regulating chondrogenesis and

osteogenesis of MSCs [44, 45], with Smad2/3 signalling known to regulate Sox9 expression [55] as well as playing a role in preventing hypertrophy [56]. It has previously been demonstrated that a low oxygen tension can increase nuclear translocation of Smad-2 and Smad-3 proteins in endothelial cells [57]. Therefore, regulation of Smad 2/3 levels and their nuclear translocation in MSCs encapsulated within DMOG releasing hydrogels is likely a downstream effect of HIF-1α stabilization which is initiated by DMOG mediated inhibition of prolyl hydroxylase domain (PHD) proteins, although future studies are required to directly confirm this link between DMOG stimulation and Smad 2/3 signalling.

To explore how these hypoxia mimicking hydrogels might influence the fate of stem cells *in vivo*, alginate hydrogels were used to co-deliver DMOG and a combination of growth factors known to support cartilage development and progression along an endochondral pathway. In our i*n vitro* evaluation of these growth factor delivery hydrogels, basal chondrogenic media without additional growth factors was used. Hence the BMP-2 and TGF-β3 that are initially loaded in the hydrogels are the only available source of growth factors for the encapsulated cells. In this model system we also found that co-delivery of DMOG will enhance chondrogenesis of MSCs, but to also enhance type X collagen expression, a common marker of hypertrophy in late-stage chondrogenesis. It should be noted, however, that *in vitro* chondrogenesis in this model system is less robust than that observed when growth factors are continuously supplemented into the culture media. When progression along the chondrogenic pathway is less advanced, the expression of markers associated with late stage chondrogenesis and hypertrophy (such as type X collagen) must be interpreted with caution, as type X collagen has previously been reported to be expressed early in chondrogenesis [58, 59]. Hence, we cannot necessarily conclude that increased type X expression early in chondrogenesis is predictive of hypertrophy later in

chondrogenesis. Importantly, we observed *in vivo* that DMOG delivery enhanced cartilage matrix accumulation and supressed calcification of the implant. In saying this, we cannot definitively conclude that DMOG delivery will prevent chondrocyte hypertrophy and endochondral ossification in the long-term, and hence further studies are required to further characterise the *in vivo* phenotype of DMOG stimulated MSCs and to examine the potential of these hypoxia mimicking hydrogels to regulate the fate of transplanted stem cells within appropriate orthotopic defect environments.

5 Conclusions

In this report, we demonstrated the ability to control the differentiation of MSCs transplanted within RGD-modified alginate hydrogels by stabilizing HIFs through the short-term release of the cell penetrating compound DMOG. Stabilization of HIFs within these MSC laden hydrogels was followed by increased nuclear localization of Smad 2/3, mimicking the intracellular signalling events observed in MSCs when maintained in low oxygen environments. As expected, based on the results of previous studies exploring the role of hypoxia in regulating MSC differentiation [3, 19, 20, 23, 60] , this resulted in increased chondrogenesis and inhibition of hypertrophy and endochondral ossification. Through the co-delivery of DMOG with recombinant growth factors, the fate of transplanted MSCs shifts to support the development of more phenotypically stable cartilaginous tissue as opposed to progressing along an endochondral pathway. The delivery of HIF-PH inhibitors to stem cells from hydrogels has numerous applications in regenerative medicine, from engineering phenotypically stable articular cartilage for synovial joint repair to spatially regulating tissue differentiation when engineering spatially complex interfaces such as the ligament-to-bone enthesis.

Data availability statement

The raw/processed data required to reproduce these findings cannot be shared at this time as the data also forms part of an ongoing study.

Acknowledgements

We express our thanks to Dr. Sreekanth Pentlavalli and Dr. Philip Chambers for providing RALA-complexed α TCP and Dr. Hannah Pauly for providing PCL nanofibrous bundles. This work was supported by a tri-partite project funded by Science Foundation Ireland (SFI), Department of Employment and Learning- Northern Ireland (DEL-NI) and the National Science Foundation (NSF) through the US-Ireland R&D Partnership Programme (USI 044, SFI-12/US/I2489), SFI 12/IA/1554 and a European Research Council Starter grant (258463).

Conflict of Interest

The authors declare no conflict of interest.

References

[1] F. Gattazzo, A. Urciuolo, P. Bonaldo, Extracellular matrix: a dynamic microenvironment for stem cell niche, Biochim Biophys Acta 1840(8) (2014) 2506-19.

[2] A. Mohyeldin, T. Garzon-Muvdi, A. Quinones-Hinojosa, Oxygen in Stem Cell Biology: A Critical Component of the Stem Cell Niche, Cell Stem Cell 7(2) (2010) 150-161.

[3] E.J. Sheehy, C.T. Buckley, D.J. Kelly, Oxygen tension regulates the osteogenic, chondrogenic and endochondral phenotype of bone marrow derived mesenchymal stem cells, Biochem Biophys Res Commun 417(1) (2012) 305-10.

[4] J. Paquet, M. Deschepper, A. Moya, D. Logeart-Avramoglou, C. Boisson-Vidal, H. Petite, Oxygen Tension Regulates Human Mesenchymal Stem Cell Paracrine Functions, Stem Cell Transl Med 4(7) (2015) 809-821.

[5] J. Leijten, N. Georgi, L. Moreira Teixeira, C.A. van Blitterswijk, J.N. Post, M. Karperien, Metabolic programming of mesenchymal stromal cells by oxygen tension directs chondrogenic cell fate, Proc Natl Acad Sci U S A 111(38) (2014) 13954-9.

[6] L.M. Swiersz, A.J. Giaccia, Z. Yun, Oxygen-dependent regulation of adipogenesis, Methods Enzymol 381 (2004) 387-95.

[7] S. Portron, V. Hivernaud, C. Merceron, J. Lesoeur, M. Masson, O. Gauthier, C. Vinatier, L. Beck, J. Guicheux, Inverse regulation of early and late chondrogenic differentiation by oxygen tension provides cues for stem cell-based cartilage tissue engineering, Cell Physiol Biochem 35(3) (2015) 841-57.

[8] E. Schipani, Hypoxia and HIF-1 alpha in chondrogenesis, Skeletal Development and Remodeling in Health, Disease, and Aging 1068 (2006) 66-73.

[9] G.L. Semenza, Hypoxia-Inducible Factors in Physiology and Medicine, Cell 148(3) (2012) 399-408.

[10] S.Y. Kim, E.G. Yang, Recent Advances in Developing Inhibitors for Hypoxia-Inducible Factor Prolyl Hydroxylases and Their Therapeutic Implications, Molecules 20(11) (2015) 20551-20568.

[11] Y. Xia, H.K. Choi, K. Lee, Recent advances in hypoxia-inducible factor (HIF)-1 inhibitors, Eur J Med Chem 49 (2012) 24-40.

[12] M. Ivan, K. Kondo, H. Yang, W. Kim, J. Valiando, M. Ohh, A. Salic, J.M. Asara, W.S. Lane, W.G. Kaelin, Jr., HIFalpha targeted for VHL-mediated destruction by proline hydroxylation: implications for O2 sensing, Science 292(5516) (2001) 464-8.

[13] P. Jaakkola, D.R. Mole, Y.M. Tian, M.I. Wilson, J. Gielbert, S.J. Gaskell, A. von Kriegsheim, H.F. Hebestreit, M. Mukherji, C.J. Schofield, P.H. Maxwell, C.W. Pugh, P.J. Ratcliffe, Targeting of HIF-alpha to the von Hippel-Lindau ubiquitylation complex by O-2-regulated prolyl hydroxylation, Science 292(5516) (2001) 468-472.

[14] A.C.R. Epstein, J.M. Gleadle, L.A. McNeill, K.S. Hewitson, J. O'Rourke, D.R. Mole, M. Mukherji, E. Metzen, M.I. Wilson, A. Dhanda, Y.M. Tian, N. Masson, D.L. Hamilton, P. Jaakkola, R. Barstead, J. Hodgkin, P.H. Maxwell, C.W. Pugh, C.J. Schofield, P.J. Ratcliffe, C-elegans EGL-9 and mammalian homologs define a family of dioxygenases that regulate HIF by prolyl hydroxylation, Cell 107(1) (2001) 43-54.

[15] T. Gomez-Leduc, M. Desance, M. Hervieu, F. Legendre, D. Ollitrault, C. de Vienne, M. Herlicoviez, P. Galera, M. Demoor, Hypoxia Is a Critical Parameter for Chondrogenic Differentiation of Human Umbilical Cord Blood Mesenchymal Stem Cells in Type I/III Collagen Sponges, Int J Mol Sci 18(9) (2017).

[16] J. Rodenas-Rochina, D.J. Kelly, J.L. Gomez Ribelles, M. Lebourg, Influence of oxygen levels on chondrogenesis of porcine mesenchymal stem cells cultured in polycaprolactone scaffolds, J Biomed Mater Res A 105(6) (2017) 1684-1691.
[17] C.T. Buckley, T. Vinardell, D.J. Kelly, Oxygen tension differentially regulates the functional properties of cartilaginous tissues engineered from infrapatellar fat pad derived MSCs and articular chondrocytes, Osteoarthritis Cartilage 18(10) (2010) 1345-54.
[18] E.G. Meyer, C.T. Buckley, S.D. Thorpe, D.J. Kelly, Low oxygen tension is a more potent promoter of chondrogenic differentiation than dynamic compression, J Biomech 43(13) (2010) 2516-23.
[19] E. Duval, C. Bauge, R. Andriamanalijaona, H. Benateau, S. Leclercq, S. Dutoit, L. Poulain, P. Galera, K. Boumediene, Molecular mechanism of hypoxia-induced chondrogenesis and its application in in vivo cartilage tissue engineering, Biomaterials 33(26) (2012) 6042-6051.
[20] N. Zhou, N. Hu, J.Y. Liao, L.B. Lin, C. Zhao, W.K. Si, Z. Yang, S.X. Yi, T.X. Fan, W. Bao, X. Liang, X. Wei, H. Chen, C. Chen, Q. Chen, X. Lin, W. Huang, HIF-1alpha as a Regulator of BMP2-Induced Chondrogenic Differentiation, Osteogenic Differentiation, and Endochondral Ossification in Stem Cells, Cell Physiol Biochem 36(1) (2015) 44-60.
[21] Z. Huang, G. He, Y. Huang, Deferoxamine synergizes with transforming growth factor-beta signaling in chondrogenesis, Genet Mol Biol 40(3) (2017) 698-702.
[22] B.L. Thoms, C.L. Murphy, Inhibition of Hypoxia-inducible Factor-targeting Prolyl Hydroxylase Domain-containing Protein 2 (PHD2) Enhances Matrix Synthesis by Human Chondrocytes, Journal of Biological Chemistry 285(27) (2010) 20472-20480.
[23] D.K. Taheem, D.A. Foyt, S. Loaiza, S.A. Ferreira, D. Ilic, H.W. Auner, A.E. Grigoriadis, G. Jell, E. Gentleman, Differential Regulation of Human Bone Marrow Mesenchymal Stromal Cell Chondrogenesis by Hypoxia Inducible Factor-1alpha Hydroxylase Inhibitors, Stem Cells (2018).
[24] N. Huebsch, P.R. Arany, A.S. Mao, D. Shvartsman, O.A. Ali, S.A. Bencherif, J. Rivera-Feliciano, D.J. Mooney, Harnessing traction-mediated manipulation of the cell/matrix interface to control stem-cell fate, Nat Mater 9(6) (2010) 518-26.
[25] O. Chaudhuri, L. Gu, D. Klumpers, M. Darnell, S.A. Bencherif, J.C. Weaver, N. Huebsch, H.P. Lee, E. Lippens, G.N. Duda, D.J. Mooney, Hydrogels with tunable stress relaxation regulate stem cell fate and activity, Nat Mater 15(3) (2016) 326-34.
[26] A. Matsiko, J.P. Gleeson, F.J. O'Brien, Scaffold mean pore size influences mesenchymal stem cell chondrogenic differentiation and matrix deposition, Tissue Eng Part A 21(3-4) (2015) 486-97.
[27] F.M. Chen, M. Zhang, Z.F. Wu, Toward delivery of multiple growth factors in tissue engineering, Biomaterials 31(24) (2010) 6279-308.
[28] P.N. Dang, N. Dwivedi, L.M. Phillips, X. Yu, S. Herberg, C. Bowerman, L.D. Solorio, W.L. Murphy, E. Alsberg, Controlled Dual Growth Factor Delivery From Microparticles Incorporated Within Human Bone Marrow-Derived Mesenchymal Stem Cell Aggregates for Enhanced Bone Tissue Engineering via Endochondral Ossification, Stem Cells Transl Med 5(2) (2016) 206-17.
[29] K.M. Park, S. Gerecht, Hypoxia-inducible hydrogels, Nat Commun 5 (2014) 4075.
[30] K.M. Park, M.R. Blatchley, S. Gerecht, The design of dextran-based hypoxia-inducible hydrogels via in situ oxygen-consuming reaction, Macromol Rapid Commun 35(22) (2014) 1968-75.
[31] C. Wu, Y. Zhou, W. Fan, P. Han, J. Chang, J. Yuen, M. Zhang, Y. Xiao, Hypoxia-mimicking mesoporous bioactive glass scaffolds with controllable cobalt ion release for bone tissue engineering, Biomaterials 33(7) (2012) 2076-85.

[32] E. Quinlan, S. Partap, M.M. Azevedo, G. Jell, M.M. Stevens, F.J. O'Brien, Hypoxia-mimicking bioactive glass/collagen glycosaminoglycan composite scaffolds to enhance angiogenesis and bone repair, Biomaterials 52 (2015) 358-66.
[33] A.L. Farris, A.N. Rindone, W.L. Grayson, Oxygen Delivering Biomaterials for Tissue Engineering, J Mater Chem B 4(20) (2016) 3422-3432.
[34] M. Gholipourmalekabadi, S. Zhao, B.S. Harrison, M. Mozafari, A.M. Seifalian, Oxygen-Generating Biomaterials: A New, Viable Paradigm for Tissue Engineering?, Trends Biotechnol 34(12) (2016) 1010-1021.
[35] E. Alsberg, H.J. Kong, Y. Hirano, M.K. Smith, A. Albeiruti, D.J. Mooney, Regulating bone formation via controlled scaffold degradation, J Dent Res 82(11) (2003) 903-908.
[36] E. Alsberg, K.W. Anderson, A. Albeiruti, R.T. Franceschi, D.J. Mooney, Cell-interactive alginate hydrogels for bone tissue engineering, J Dent Res 80(11) (2001) 2025-9.
[37] J.A. Rowley, G. Madlambayan, D.J. Mooney, Alginate hydrogels as synthetic extracellular matrix materials, Biomaterials 20(1) (1999) 45-53.
[38] C. Wu, Y. Zhou, J. Chang, Y. Xiao, Delivery of dimethyloxallyl glycine in mesoporous bioactive glass scaffolds to improve angiogenesis and osteogenesis of human bone marrow stromal cells, Acta Biomater 9(11) (2013) 9159-68.
[39] C.A. Simmons, E. Alsberg, S. Hsiong, W.J. Kim, D.J. Mooney, Dual growth factor delivery and controlled scaffold degradation enhance in vivo bone formation by transplanted bone marrow stromal cells, Bone 35(2) (2004) 562-9.
[40] T.D. Schmittgen, K.J. Livak, Analyzing real-time PCR data by the comparative C(T) method, Nat Protoc 3(6) (2008) 1101-8.
[41] B.N. Sathy, D. Olvera, T. Gonzalez-Fernandez, G.M. Cunniffe, S. Pentlavalli, P. Chambers, O. Jeon, E. Alsberg, H.O. McCarthy, N. Dunne, RALA complexed α-TCP nanoparticle delivery to mesenchymal stem cells induces bone formation in tissue engineered constructs in vitro and in vivo, Journal of Materials Chemistry B 5(9) (2017) 1753-1764.
[42] C.T. Buckley, T. Vinardell, S.D. Thorpe, M.G. Haugh, E. Jones, D. McGonagle, D.J. Kelly, Functional properties of cartilaginous tissues engineered from infrapatellar fat pad-derived mesenchymal stem cells, Journal of Biomechanics 43(5) (2010) 920-926.
[43] J. Zhang, J. Guan, X. Qi, H. Ding, H. Yuan, Z. Xie, C. Chen, X. Li, C. Zhang, Y. Huang, Dimethyloxaloylglycine Promotes the Angiogenic Activity of Mesenchymal Stem Cells Derived from iPSCs via Activation of the PI3K/Akt Pathway for Bone Regeneration, Int J Biol Sci 12(6) (2016) 639-52.
[44] H. Ding, S. Chen, W.Q. Song, Y.S. Gao, J.J. Guan, Y. Wang, Y. Sun, C.Q. Zhang, Dimethyloxaloylglycine improves angiogenic activity of bone marrow stromal cells in the tissue-engineered bone, Int J Biol Sci 10(7) (2014) 746-56.
[45] M.R. Wu, G.Q. Chen, Y.P. Li, TGF-beta and BMP signaling in osteoblast, skeletal development, and bone formation, homeostasis and disease, Bone Res 4 (2016).
[46] P. Malladi, Y. Xu, M. Chiou, A.J. Giaccia, M.T. Longaker, Effect of reduced oxygen tension on chondrogenesis and osteogenesis in adipose-derived mesenchymal cells, Am J Physiol Cell Physiol 290(4) (2006) C1139-46.
[47] J. Massague, J. Seoane, D. Wotton, Smad transcription factors, Gene Dev 19(23) (2005) 2783-2810.
[48] R. Derynck, Y.E. Zhang, Smad-dependent and Smad-independent pathways in TGF-beta family signalling, Nature 425(6958) (2003) 577-84.

[49] G.M. Cunniffe, T. Gonzalez-Fernandez, A. Daly, B.N. Sathy, O. Jeon, E. Alsberg, D.J. Kelly, * Three-Dimensional Bioprinting of Polycaprolactone Reinforced Gene Activated Bioinks for Bone Tissue Engineering, Tissue Eng Part A 23(17-18) (2017) 891-900.
[50] L.K. Nguyen, M.A. Cavadas, C.C. Scholz, S.F. Fitzpatrick, U. Bruning, E.P. Cummins, M.M. Tambuwala, M.C. Manresa, B.N. Kholodenko, C.T. Taylor, A. Cheong, A dynamic model of the hypoxia-inducible factor 1alpha (HIF-1alpha) network, J Cell Sci 126(Pt 6) (2013) 1454-63.
[51] H.H. Tonnesen, J. Karlsen, Alginate in drug delivery systems, Drug Dev Ind Pharm 28(6) (2002) 621-30.
[52] B.H. Jiang, G.L. Semenza, C. Bauer, H.H. Marti, Hypoxia-inducible factor 1 levels vary exponentially over a physiologically relevant range of O2 tension, Am J Physiol 271(4 Pt 1) (1996) C1172-80.
[53] M. Kanichai, D. Ferguson, P.J. Prendergast, V.A. Campbell, Hypoxia promotes chondrogenesis in rat mesenchymal stem cells: a role for AKT and hypoxia-inducible factor (HIF)-1alpha, J Cell Physiol 216(3) (2008) 708-15.
[54] J.C. Robins, N. Akeno, A. Mukherjee, R.R. Dalal, B.J. Aronow, P. Koopman, T.L. Clemens, Hypoxia induces chondrocyte-specific gene expression in mesenchymal cells in association with transcriptional activation of Sox9, Bone 37(3) (2005) 313-22.
[55] S. Itoh, F. Itoh, M.J. Goumans, P. Ten Dijke, Signaling of transforming growth factor-beta family members through Smad proteins, Eur J Biochem 267(24) (2000) 6954-67.
[56] X. Yang, L. Chen, X. Xu, C. Li, C. Huang, C.X. Deng, TGF-beta/Smad3 signals repress chondrocyte hypertrophic differentiation and are required for maintaining articular cartilage, J Cell Biol 153(1) (2001) 35-46.
[57] H. Zhang, H.O. Akman, E.L.P. Smith, J. Zhao, J.E. Murphy-Ullrich, M.A.Q. Siddiqui, O.A. Batuman, Cellular response to hypoxia involves signaling via Smad proteins, Blood 101(6) (2003) 2253-2260.
[58] F. Mwale, D. Stachura, P. Roughley, J. Antoniou, Limitations of using aggrecan and type X collagen as markers of chondrogenesis in mesenchymal stem cell differentiation, J Orthop Res 24(8) (2006) 1791-8.
[59] K. Pelttari, A. Winter, E. Steck, K. Goetzke, T. Hennig, B.G. Ochs, T. Aigner, W. Richter, Premature induction of hypertrophy during in vitro chondrogenesis of human mesenchymal stem cells correlates with calcification and vascular invasion after ectopic transplantation in SCID mice, Arthritis Rheum 54(10) (2006) 3254-66.
[60] J. Leijten, N. Georgi, L.M. Teixeira, C.A. van Blitterswijk, J.N. Post, M. Karperien, Metabolic programming of mesenchymal stromal cells by oxygen tension directs chondrogenic cell fate, P Natl Acad Sci USA 111(38) (2014) 13954-13959.

Figure Legends

Fig.1: Development and evaluation of HIF-stabilizing hydrogels. (A) Cumulative release of DMOG from the RGD-Alginate hydrogels with 3 different concentrations of DMOG (2.1, 4.2 and 6.3 mg/mL). (B) Representative Live/ Dead staining of MSCs encapsulated in the hydrogels after 24h of *in vitro* culture at 5% O_2 (Green = Live cells, Red = Dead cells). (C) Representative confocal images of MSCs encapsulated in RGD-Alginate (control) and DMOG releasing RGD-Alginate (4.2 mg DMOG /mL) hydrogels recovered from the hydrogels and immuno-stained against HIF-1α after 2h *in vitro,* at both 20% and 5% oxygen. (D) Quantification of the ratio of nuclear to cytoplasmic HIF-1 α in MSCs maintained at 20 % and 5% oxygen conditions after 2 h. (E) Western blot analysis of HIF-1α levels in MSCs 24 h after encapsulation within control hydrogels and DMOG releasing (2.1, 4.2 and 6.3 mg/mL) hydrogels at 20% and 5% oxygen.

Fig. 2: Expression of chondrogenic, hypertrophic and osteogenic genes in MSCs after 1 week of culture and matrix deposition after 3 weeks of culture in the control and DMOG releasing hydrogels maintained in 20% and 5% oxygen conditions in the presence of TGF β3. (A, B) Quantification of gene expression after 1 week of culture at 20% and 5% oxygen. Expression is relative to that in control (DMOG-free) hydrogels maintained at 20% or 5% oxygen respectively. '*' indicates $P< 0.05$ (upregulation) and '+' indicates $P< 0.05$ (downregulation) compared to untreated controls (n = 3). (C) Aldehyde fuchsin/alcian blue and picrosirius red stained sections from hydrogels maintained at 20% oxygen demonstrating GAG and collagen deposition respectively. (D) Biochemical quantification of GAG synthesis in hydrogels maintained at 20% oxygen. *$P< 0.05$ compared to untreated control (n = 5). (E) Aldehyde fuchsin/alcian blue and picrosirius red stained sections from hydrogels maintained at 5% oxygen showing demonstrating

GAG and collagen deposition respectively. (F) Biochemical quantification of GAG synthesis in hydrogels which were maintained at 5% oxygen. (G) Type-II collagen immunostaining in DMOG releasing hydrogels compared to control hydrogels at 20% and 5% oxygen conditions at week 3. Scale bar = 500 µm (low magnification images).

Fig. 3: Protein expression and the nuclear translocation of Smad 2/3 in MSCs encapsulated in DMOG releasing hydrogels. (A and B) representative confocal microscopic images of MSCs encapsulated in the hydrogels recovered from the hydrogels and immunostained against Smad 2/3 and counter stained with DAPI after 48 h incubation at 20% and 5% O_2 respectively. (C) Mean Smad 2/3 signal intensity in the cytosol and nucleus, as well as the Smad 2/3 nuclear to cytoplasmic ratio, in control (DMOG-free) hydrogels maintained at 20% and 5% oxygen. (D and E) Mean Smad 2/3 signal intensity in the cytosole and nucleus, as well as the Smad 2/3 nuclear to cytoplasmic ratio in MSCs encapsulated in control and DMOG releasing hydrogels at 20% oxygen and 5 % oxygen respectively.

Fig. 4: Effect of DMOG and GF co-delivery from hydrogels on the chondrogenic differentiation of encapsulated MSCs *in vitro*. (A, B) Relative quantification of chondrogenic gene expression after 1 week in hydrogels maintained at 20% and 5% O_2. Expression is relative to that within control hydrogels (free of DMOG and GF) maintained at 20% or 5% oxygen respectively. (C) Aldehyde fuchsin/alcian blue stained sections demonstrating GAG accumulation. (D) Biochemical quantification of GAG and collagen synthesis in the hydrogels. '*' indicates $P < 0.05$ compared to untreated controls (n = 5).

Fig. 5: Effect of DMOG + GF co-delivery from alginate hydrogels containing MSCs on chondrogenesis and mineralization *in vivo*. (A) Haematoxylin eosin, aldehyde fuchsin/alcian blue stained sections and type-I, type- II and type-X collagen immuno stained sections obtained from

DMOG + GF co-delivery hydrogels and control hydrogels (GF only) after 4 weeks *in vivo*. (B) Hematoxylin eosin, Goldner's trichrome, aldehyde fuchsin/alcian blue and alizarin red stained sections and representative micro-CT images of DMOG incorporated-GF delivery hydrogels and control hydrogels (GF only) after 12 weeks *in vivo*. (C) Biochemical quantification of GAG content in the hydrogels after 12 weeks *in vivo*. (D) Micro-CT quantification of the mineral volume at 12 weeks. *P< 0.05 compared to GF only hydrogels (n = 5).

Table-1

Genes and primer sequences used for quantitative real-time PCR analysis

Fig.1

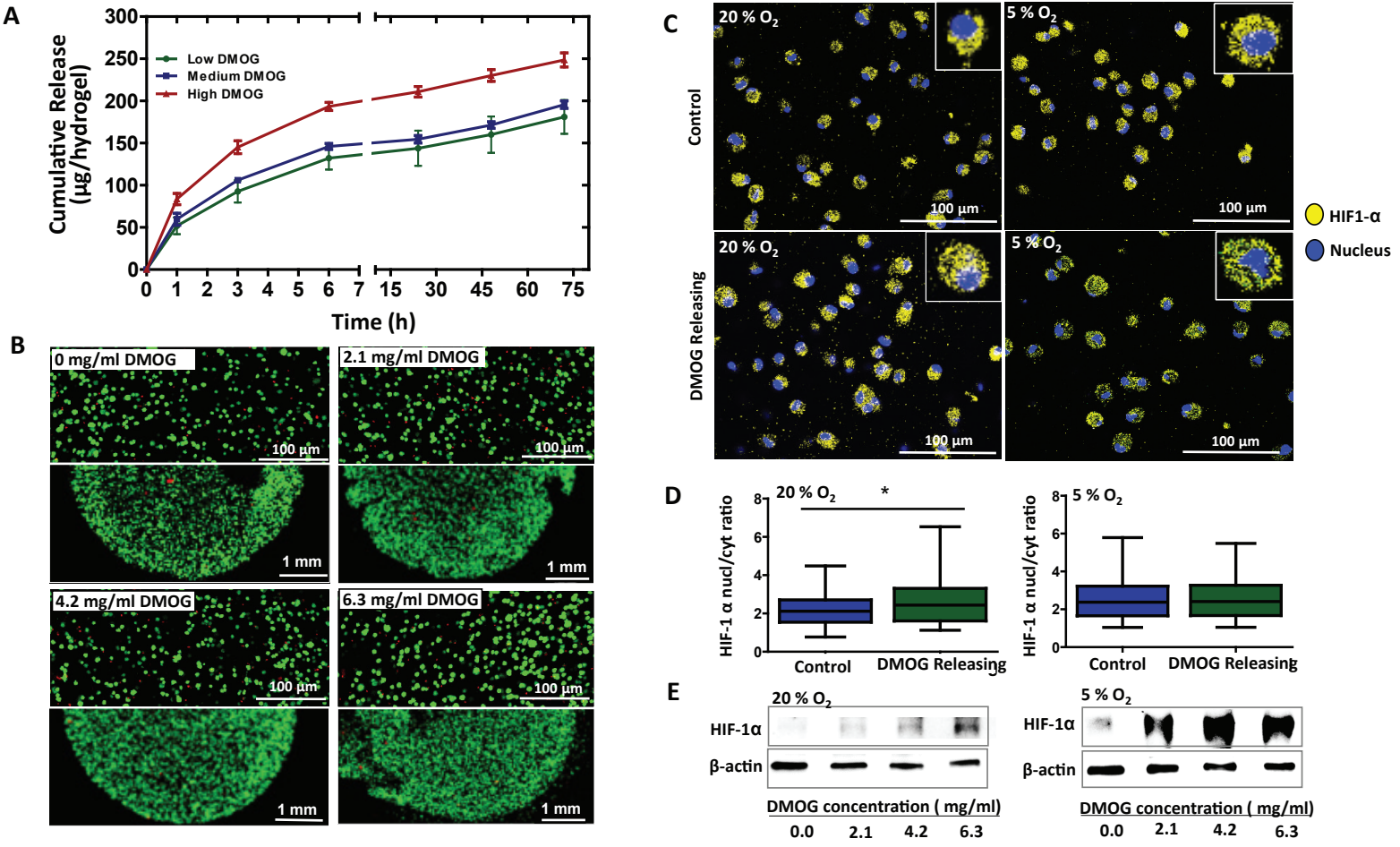
A
Cumulative Release (μg/hydrogel)
Low DMOG
Medium DMOG
High DMOG
Time (h)
B
0 mg/ml DMOG
2.1 mg/ml DMOG
4.2 mg/ml DMOG
6.3 mg/ml DMOG
100 μm
1 mm
C
20 % O2
5 % O2
Control
DMOG Releasing
HIF1-α
Nucleus
D
HIF-1 α nucl/cyt ratio
*
Control
DMOG Releasing
E
HIF-1α
β-actin
DMOG concentration (mg/ml)
0.0
2.1
4.2
6.3

Fig.2

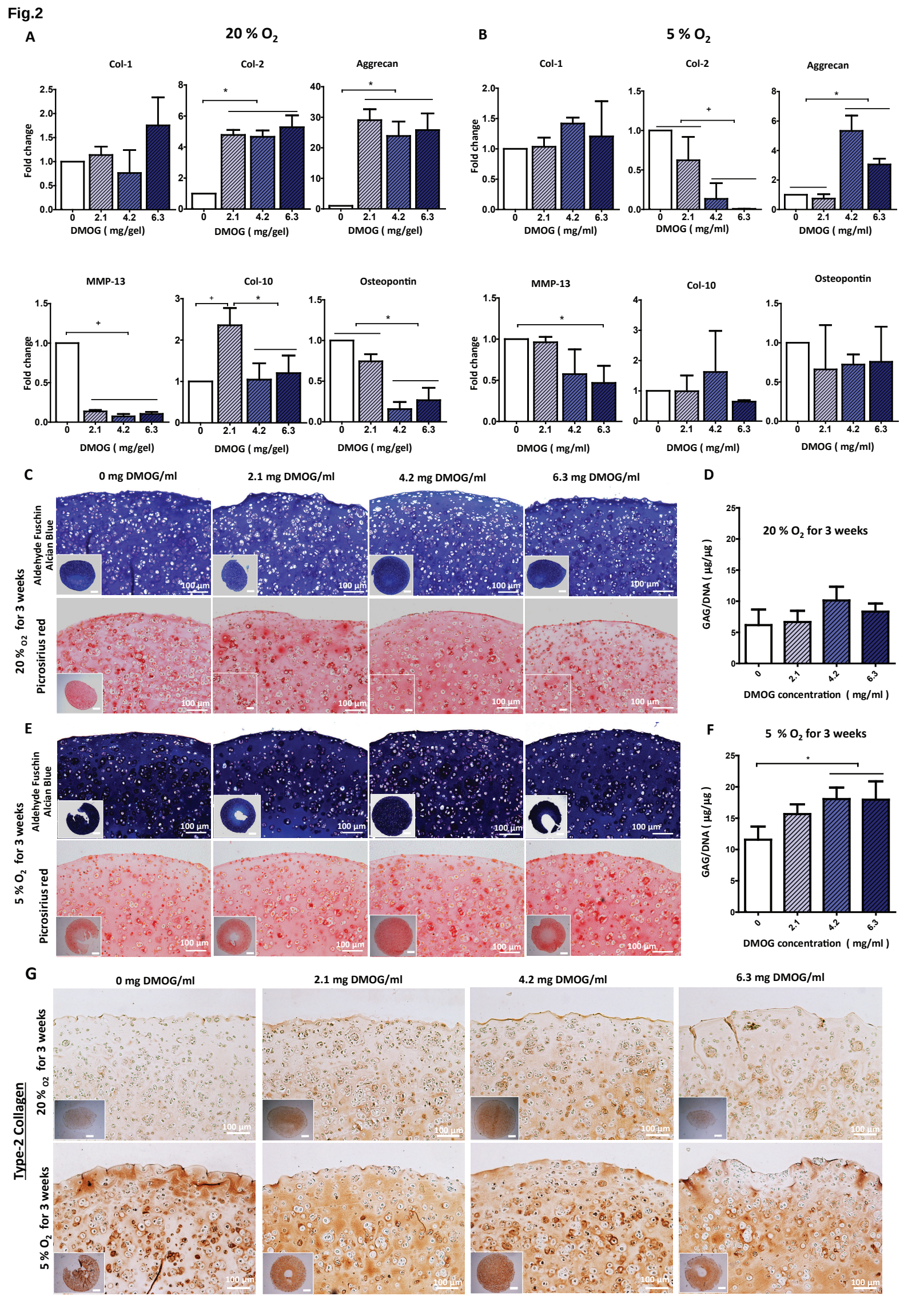
A
20 % O2
Col-1
Col-2
Aggrecan
MMP-13
Col-10
Osteopontin
Fold change
DMOG (mg/gel)
B
5 % O2
DMOG (mg/ml)
C
0 mg DMOG/ml
2.1 mg DMOG/ml
4.2 mg DMOG/ml
6.3 mg DMOG/ml
20 % O2 for 3 weeks
Aldehyde Fuschin Alcian Blue
Picrosirius red
100 µm
D
20 % O2 for 3 weeks
GAG/DNA (µg/µg)
DMOG concentration (mg/ml)
E
5 % O2 for 3 weeks
F
5 % O2 for 3 weeks
G
Type-2 Collagen

Fig.3

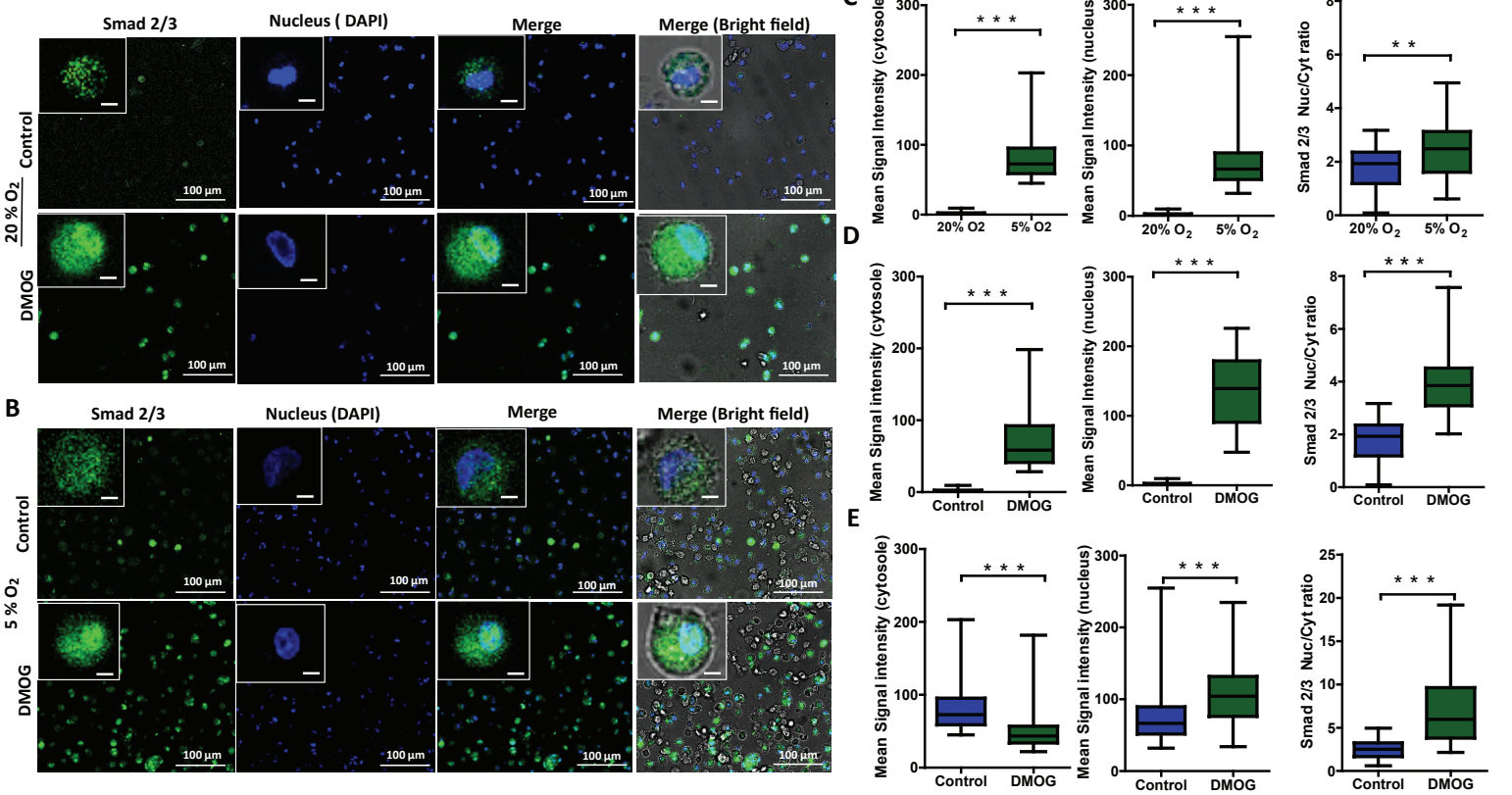
A
Smad 2/3
Nucleus (DAPI)
Merge
Merge (Bright field)
Control
DMOG
20 % O2
100 µm
B
Smad 2/3
Nucleus (DAPI)
Merge
Merge (Bright field)
Control
DMOG
5 % O2
100 µm
C
Mean Signal Intensity (cytosole)
Mean Signal Intensity (nucleus)
Smad 2/3 Nuc/Cyt ratio
* * *
* *
20% O2
5% O2
20% O2
5% O2
D
Mean Signal intensity (cytosole)
Mean Signal Intensity (nucleus)
Smad 2/3 Nuc/Cyt ratio
* * *
Control
DMOG
E
Mean Signal intensity (cytosole)
Mean Signal intensity (nucleus)
Smad 2/3 Nuc/Cyt ratio
* * *
Control
DMOG

Fig.4

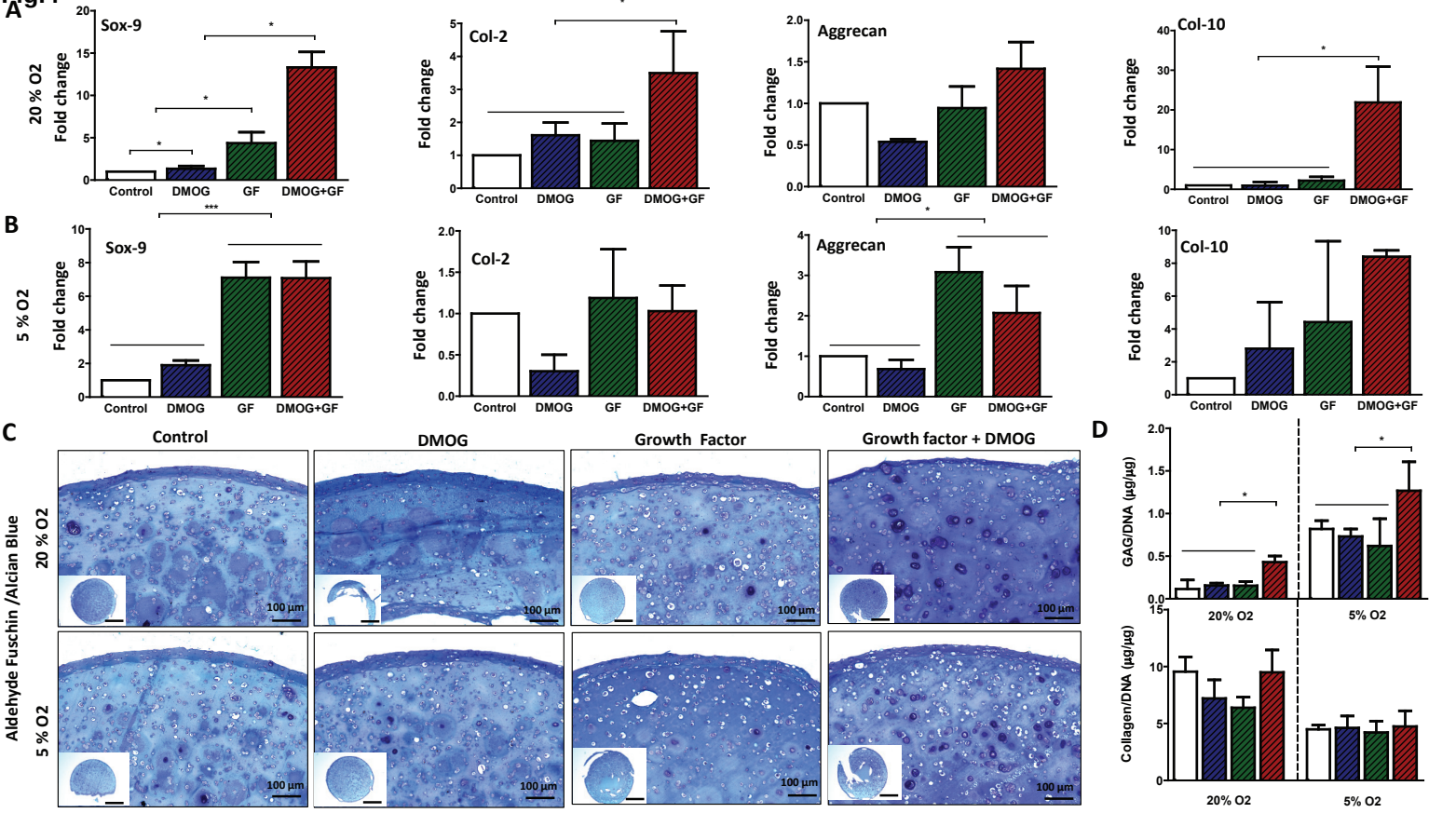
A
20 % O2
Sox-9
Col-2
Aggrecan
Col-10
Fold change
Control
DMOG
GF
DMOG+GF
B
5 % O2
C
Control
DMOG
Growth Factor
Growth factor + DMOG
Aldehyde Fuschin /Alcian Blue
100 µm
D
GAG/DNA (µg/µg)
Collagen/DNA (µg/µg)
20% O2
5% O2

Fig.5

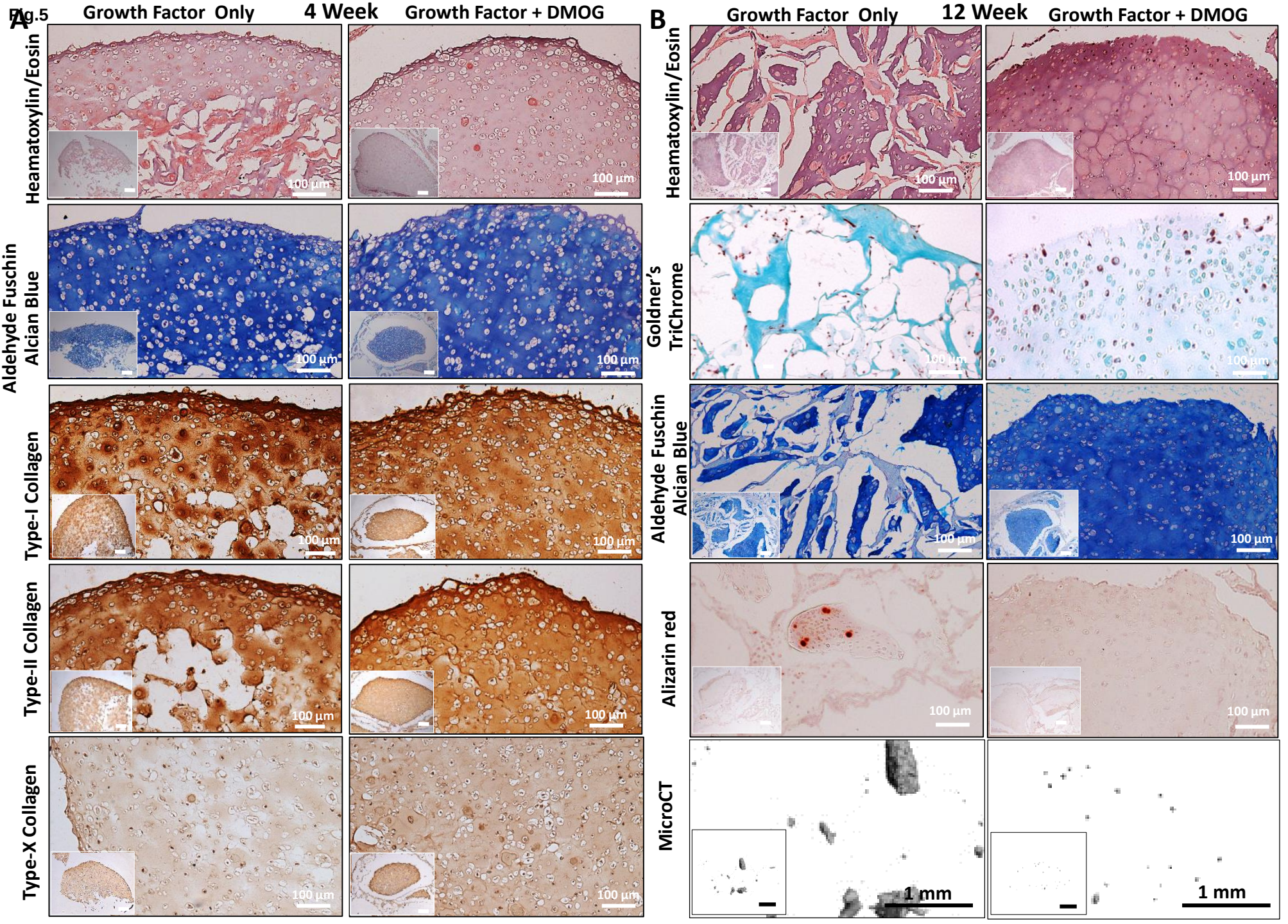
A
Growth Factor Only
4 Week
Growth Factor + DMOG
Heamatoxylin/Eosin
Aldehyde Fuschin Alcian Blue
Type-I Collagen
Type-II Collagen
Type-X Collagen
100 µm
B
Growth Factor Only
12 Week
Growth Factor + DMOG
Heamatoxylin/Eosin
Goldner's TriChrome
Aldehyde Fuschin Alcian Blue
Alizarin red
MicroCT
100 µm
1 mm

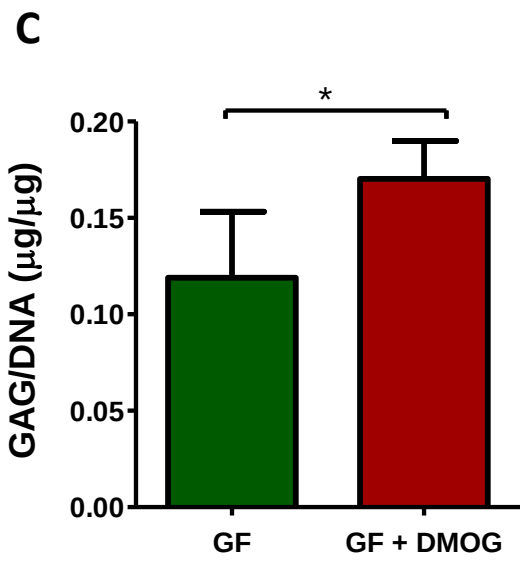
C
GAG/DNA (µg/µg)
0.20
0.15
0.10
0.05
0.00
*
GF
GF + DMOG

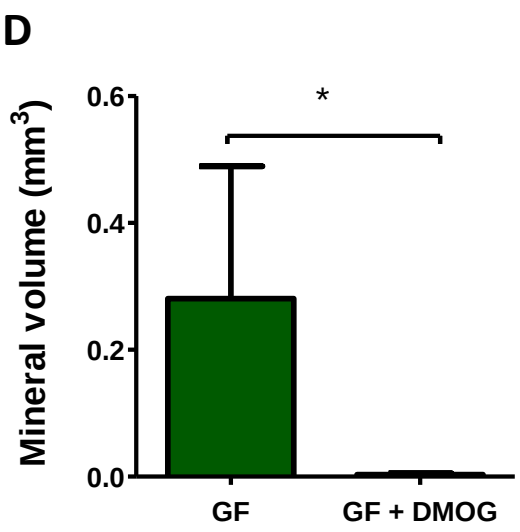
D
Mineral volume (mm3)
0.6
0.4
0.2
0.0
*
GF
GF + DMOG

Table

Gene	Symbol	Forward Primer	Reverse Primer
Collagen type-1	Col-1A1	TAGACATGTTCAGCTTTGTG	GTGGGATGTCTTCTTCTTG
Collagen type- 2	Col-2A1	CGACGACATAATCTGTGAAG	TCCTTTGGGTCCTACAATATC
Collagen type-10	Col-10A1	GTAGGTGTTTGGTATTGCTC	GAGCAATACCAAACACCTAC
Aggrecan	ACAN	GACCACTTTACTCTTGGTG	TCAGGCTCAGAAACTTCTAC
Matrix metallopeptidase 13	MMP-13	GACCAAATTATGGAGGAGATG	AAACAAGTTGTAGCCTTTGG
Secreted phosphoprotein 1 (Osteopontin)	SPP1	CTGCAGACCAAGGAAAATC	AGCATCTGTGTATTTGTTGG
SRY (Sex Determining Region Y)-Box-9	SOX9	CAGACCTTGAGGAGACTTAG	GTTCGAGTTGCCTTTAGTG
Glyceraldehyde-3-phosphate dehydrogenase	GAPDH	TTTAACTCTGGCAAAGTGG	GAACATGTAGACCATGTAGTG

Supplementary Material

Click here to download Supplementary Material: Supplementary Figure_1.pdf

Supplementary Material

Click here to download Supplementary Material: Supplimentary Figure_2.pdf